Cai *et al. J Wireless Com Network* (2024) 2024:17
https://doi.org/10.1186/s13638-024-02344-w

EURASIP Journal on Wireless Communications and Networking

RESEARCH Open Access

Energy-efficient two-way full-duplex relay transmission strategy with SWIPT and direct links

Caixia Cai[1*], Fuli Zhong[2], Han Hai[3], Mingzhi Chen[4], Wenyang Gan[1], Bing Sun[1] and Yayu Yang[1]

*Correspondence:
cxcai@shmtu.edu.cn

[1] Department of Electrical Engineering, Shanghai Maritime University, Shanghai 201306, China
[2] School of Systems Science and Engineering, Sun Yat-Sen University, Guangzhou 510006, China
[3] College of Information Sciences and Technology, Donghua University, Shanghai 201620, China
[4] School of Mechanical Engineering, University of Shanghai for Science and Technology, Shanghai 200093, China

Abstract

In this paper, we improve networks' spectral efficiency (SE), extend networks' lifetime, and maximize networks' energy efficiency (EE) of two-way full-duplex (FD) relay networks. Firstly, to improve networks' SE and to extend networks' lifetime simultaneously, we design a two-way FD relay transmission strategy with simultaneous wireless information and power transfer and direct links (DLs). The designed transmission strategy can complete a bidirectional communication in only one time slot with the exists of DLs and the energy-constrained relay node. With the designed transmission strategy, we further give the characteristics of relay amplification factor, the analysis of the designed transmission strategy, and the EE analysis of traditional half-duplex two-way amplify-and-forward relaying. Secondly, to maximize networks' EE, we present both the EE maximization problems and analyses of the designed transmission strategy with equal power allocation and optimal power allocation. To solve the EE maximization problems, we further propose the alternating optimal algorithm and give complexity analysis of the algorithm. Simulations show that our designed transmission strategy can improve the SE and EE of the networks.

Keywords: Two-way relaying, Full-duplex, Simultaneous wireless information and power transfer, Direct links, Energy efficiency

1 Introduction

Wireless networks affect all aspects of our daily lives for their ever growing and emerging applications, such as vehicle Ad Hoc networks, IoT networks, some industrial networks and so on. However, the operational time of energy-constrained devices usually limits the wireless networks' lifetime [1]. To address this problem, there introduce different energy harvesting (EH) techniques. Simultaneous wireless information and power transfer (SWIPT) is a sustainable solution to the scenarios where replacing or recharging batteries is very costly or hardly [2]. The SWIPT can use the received radio frequency signals to keep energy-constrained devices operational. Existing studies adopt time-switching (TS) and power-splitting (PS) protocols to implement a SWIPT receiver architecture. The TS and PS protocols can use one part of segregated resources for information decoding (ID), and the other for EH. In particular, the [3] considered joint

transmit power and TS control in SWIPT cellular networks to maximize throughput, and the [4] studied resource allocation in a underlaid cellular networks to maximize energy efficiency (EE). Both of the [3] and [4] can extend the networks' lifetime. Because the energy-constrained node can harvest energy from the received signal.

Relay technique can improve reliability, enhance spectral efficiency (SE), and improve connectivity of wireless networks [5, 6]. The [7] and [8] also proved that the relay technique can improve the security of wireless networks. This means the relay technique can play an important role in wireless networks for its varieties of advantages. The integration of the SWIPT into relay networks can expand communication range and keep energy-constrained nodes active simultaneously. The [9] and [10] studied the wireless-powered relay networks with TS-based relaying and/or PS-based relaying. Specifically, the [9] maximized the EE of the energy-constrained multi-relay networks. Moreover, the [10] studied the PS based one-way relaying to improve outage performance. Furthermore, the [11] examined the transmission performance with non-coherent modulation by considering both TS-based and PS-based amplify-and-forward (AF) relay protocols. The [9–11] showed the benefits of combing the SWIPT and the relay technique effectively.

However, the [9–11] only considered the one-way relaying. This means they suffered from SE loss to some extent with two time slots to achieve a one-way communication [12]. To make up for this deficiency, two-way relaying (TWR) becomes popular and this paper also considers the TWR. By combining the SWIPT and the TWR, the [13] proposed a PS ratio optimization scheme to maximize EE and the [14] proposed a dynamic asymmetric PS scheme to minimize outage probability. However, the [13] and [14] only considered the half-duplex (HD) transceivers. Therefore, they still partly suffered from SE loss to some extent. Fortunately, the [15–17] proved that the full-duplex (FD) technique can overcome this inherent SE loss with the technological progress in self-interference cancellation (SIC) techniques.

Considering the SE advantages of the TWR and the FD technique, the integration of the TWR and the FD technique receives a lot of attention in recent years. For example, the [18] investigated a multiuser TWR system with FD technique to improve average rate, and the [19] analyzed relay power optimization with FD technique to improve SE. However, both the [18] and [19] did not consider the energy-constrained problem. To consider the TWR system with the FD technique and the SWIPT, the [20] and [21] discussed the problem of relay selection. The [20] and [21] also showed their SE and outage probability superiorities of the TWR system with the FD technique and the SWIPT. But the [20] and [21] focused on the problem of relay selection to maximize capacity. At the same time, they were limited to the simplified system model. In the simplified system model, it usually ignores the direct links (DLs) in relay transmission. Actually, the DLs in relay transmission can achieve further SE performance gain [22]. Because the DLs in relay transmission also can convey information, and some works have shown this property. For example, the [22] discussed the optimal design of source and relay nodes with DLs to against channel state information (CSI) errors, and the [23] studied bidirectional relay transmissions with DLs to improve EE.

Based on the above analysis, we can get three important points. First, the TWR, the FD technique, and the DLs in relay transmission can improve the networks' SE. While

the combination of the three can further improve the networks' SE. Second, the SWIPT can extend the networks' lifetime. Because the energy-constrained node can harvest energy from the received signal. Third, it seems that there is no effort to consider the TWR, the FD technique, the DLs in relay transmission, and the SWIPT in one paper to improve networks' SE and to extend networks' lifetime, simultaneously.

At the same time, except for the networks' SE and the networks' lifetime, the networks' EE is also a very important performance metric for the wireless networks [24]. Thus, the related works also investigated the EE maximization problem. For example, authors in [25] and [12] respectively studied the EE maximization problem in two-way HD and FD relay networks without considering SWIPT architecture, and authors in [13] and [15] respectively examined the EE maximization problem in two-way HD and FD relay networks with considering SWIPT architecture. However, to the best of the authors' knowledge, there is still no effort in open literature to investigate the EE maximization problem with the integration of the TWR, the FD technique, the DLs in relay transmission, and the SWIPT. Namely, to consider the TWR, the FD technique, the DLs in relay transmission, the SWIPT, and the EE maximization problem, five characteristics in one paper.

Improving networks' SE, extending networks' lifetime, and maximizing networks' EE is a promising solution to meet the requirements of future wireless networks, which is still relatively under-explored. Motivated by the limitations of the related works with only consider part of the five characteristics in Table 1, this paper attempts to meet the requirements of future wireless networks with our proposed two-way FD relay transmission strategy. The contributions of this paper are summarized as follows:

- To improve networks' SE and to extend networks' lifetime simultaneously, this paper designs a transmission strategy with the integration of the TWR, the FD technique, the DLs in relay transmission, and the SWIPT. With the designed transmission strategy, this paper further gives the characteristics of relay amplification factor, the analysis of the designed transmission strategy, and the EE analysis of traditional HD two-way AF relaying.

Table 1 Related Literatures' Considered Characteristics

Related literatures	FD	TWR	DL	SWIPT	EE
[4, 9, 11]				✓	✓
[10]			✓	✓	
[12]	✓	✓			
[13]		✓		✓	✓
[14]		✓		✓	
[15]	✓	✓		✓	✓
[18, 19]	✓	✓			
[20, 21]	✓	✓		✓	
This paper	✓	✓	✓	✓	✓

- To maximize networks' EE, this paper presents both the EE maximization problems and analyses of the designed transmission strategy with equal power allocation (EPA) and optimal power allocation (OPA).
- To solve the EE maximization problems, this paper further proposes the alternating optimal algorithm and gives the algorithm complexity analysis of the algorithm. For simplicity, we express the designed transmission strategy as FD-TWR-SWIPT-DL transmission strategy in the following parts.

2 System model

Consider the traditional two-way AF relay networks [6] consisting of two FD end nodes S_1 and S_2 and one FD relay node R. All the nodes are equipped with a transmit antenna and a receive antenna, and operated in the FD mode during the time slot 1. Figure 1 shows the transmission model of the FD-TWR-SWIPT-DL transmission strategy and it is similar to [12]. However, the [12] assumed all the signals forwarded by the relay as unit signals. Although this assumption can help the [12] to simplify the analysis and get the analytical expression of OPA. But it also brings some problems. For example, it cannot make full use of the AF relay protocol's characteristics to get the relay gain. Except for this assumption, there are also two differences between this paper and the [12]. Firstly, there exists DLs between two end nodes and the DLs can transmit signal in this paper. Secondly, the relay node transmits signal with SWIPT to extend networks' lifetime in this paper. As in Fig. 2, the power splitter at the relay node divides the received signal into an information decoder with α portion and an energy harvester with $(1-\alpha)$ portion [14]. This paper considers the EH model of SWIPT-PS for its superiority of hardware features. The Fig. 2 shows the nodes' signal transmission model of the FD-TWR-SWIPT-DL transmission strategy.

The channels h_i, h_j, and h experience independent quasi-static Rayleigh fading and remain unchanged within the fixed duration of one frame $T = 5$ ms [25, 26]. The h_i (or h_j) is the channel between node S_i (or S_j) and R, h is the channel between node S_i and S_j, where $\{i,j\} \in \{1,2\}$ and $i \neq j$, namely, $i = 1, j = 2$ or $i = 2, j = 1$. The channels between the same two nodes are also reciprocal. The $\widetilde{h_{ii}}$ (or $\widetilde{h_{jj}}$) is the residual self-interference (RSI) channel at node S_i (or S_j), $\widetilde{h_{rr}}$ is the RSI channel at node R. The RSI channels $\widetilde{h_{ii}}$, $\widetilde{h_{jj}}$, and $\widetilde{h_{rr}}$ are subject to independent Ricean fading at different frames. The average power gains of the RSI channels are $\mathbb{E}\{|\widetilde{h_{ii}}|^2\} = \Omega_i$ and $\mathbb{E}\{|\widetilde{h_{rr}}|^2\} = \Omega_r$. All nodes only know the statistical characterization of the RSI channels, i.e., Ω_i and Ω_r [27]. We assume that there exists a central processor in the networks. The central processor can access to all CSIs and other required information for processing signal. At the same time, this processor feeds back the calculated data to all the networks nodes and help all the nodes to receive and forward signal [12]. The transmit signal of the node S_i is x_i with $\mathbb{E}\{|x_i|^2\} = 1$ and $\mathbb{E}\{x_i\} = 0$. The node S_i combines the received signals with maximum ratio combining (MRC) technique. The noises at three nodes are zero-mean symmetric complex Gaussian vector with variance σ^2.

2.1 Total capacity and energy consumption models

The total capacity contains the transmission tasks in two directions with a round of bidirectional communication [25]. Then, as [12, 23, 25], the total capacity of the FD-TWR-SWIPT-DL transmission strategy is

$$C_t = C_1 + C_2, \tag{1}$$

where C_1 and C_2 are the capacities in two directions.

The total energy consumption contains transmit powers and circuit powers [12]. At the same time, the power amplifier usually works in non-ideal environment with the features of hardware. Thus, the power amplifier efficiency should be considered to show the actually transmit powers consumption [13]. Then, the total energy consumption of the FD-TWR-SWIPT-DL transmission strategy is

$$E_t = T^t(\epsilon P^t + P^c), \tag{2}$$

where $1/\epsilon$ is power amplifier efficiency, T^t is transmit time and $T^t \in (0, T]$. The P^t is the total transmit power and the P^c is the total circuit power.

2.2 Problem formulation

To improve networks' SE and to extend networks' lifetime simultaneously, this paper designs the FD-TWR-SWIPT-DL transmission strategy. With the FD-TWR-SWIPT-DL transmission strategy, this paper attempts to present both the EE maximization problems and analyses with EPA and OPA. Based on the total capacity and total energy consumption models, this paper defines the EE as the ratio of total transmission bits to total consumed energy, and it is $\eta = \frac{C_t}{E_t}$ [24, 25]. It means that this paper needs to maximize the η of the FD-TWR-SWIPT-DL transmission strategy with EPA and OPA.

3 Methods

In this section, we give the details of the FD-TWR-SWIPT-DL transmission strategy and the method to maximize the EE of it.

3.1 Transmission strategy design and analysis

In this subsection, we give the design and analysis of the FD-TWR-SWIPT-DL transmission strategy.

3.1.1 Transmission strategy design

Firstly, we give the design of the FD-TWR-SWIPT-DL transmission strategy. Figures 1 and 2 respectively show the specific transmission model and nodes' signal transmission model.

From Fig. 1, we can see that the FD-TWR-SWIPT-DL transmission strategy can complete the information exchange between the two nodes S_1 and S_2 in only one time slot. In the only one time slot, all the nodes transmit and receive signal with FD transceivers. As it has been stated in [16] that the self-interference at the FD transceivers can be canceled by jointly using three-step interference cancelation, i.e., antenna, analog, and digital interference cancelations. However, even with the SIC, the self-interference cannot be canceled completely [12]. Thus, all the nodes have RSI and the RSI is considered in this paper. At the same time, there exists DLs between two nodes S_1 and S_2. So the nodes S_1 and S_2 can respectively transmit $x_1(m)$ and $x_2(m)$ in frame m to each other. What's more, the FD relay node is an energy-constrained node and it forwards the received signal $x_r(m)$ with only α portion.

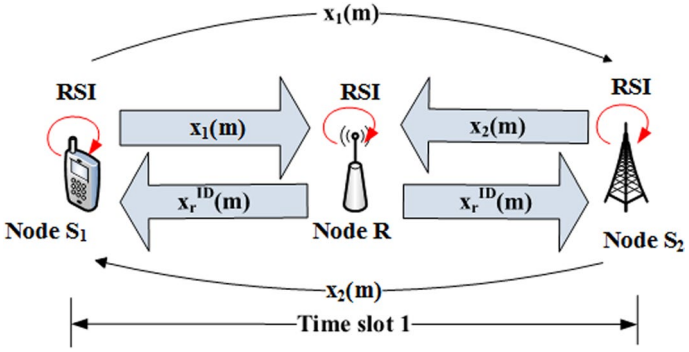

Fig. 1 Transmission model of FD-TWR-SWIPT-DL transmission strategy

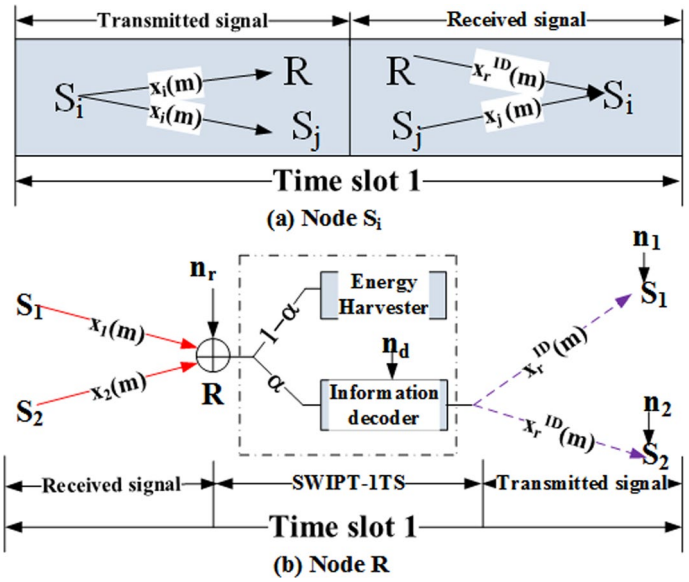

Fig. 2 Nodes' signal transmission model **a** Node S_i; **b** Node R

From Fig. 2, we can see the transmitted and received signals of node S_i and R. Figure 2a gives the signal transmission model of node S_i. For node S_i, it transmits signal $x_i(m)$ to node S_j and R. At the same time, it receives signal $x_j(m)$ from node S_j, and it receives signal $x_r^{ID}(m)$ from node R. Then, with SIC and MRC techniques, the received signal at node S_i is

$$y_i(m) = h_i x_r^{ID}(m) + \sqrt{P_j^t} h x_j(m) + \sqrt{P_i^t}\widetilde{h_{ii}}(m) x_i(m) + n_i, \tag{3}$$

where $\sqrt{P_i^t}\widetilde{h_{ii}}(m)x_i(m)$ is the RSI at the node S_i, $h_i x_r^{ID}(m)$ is the relay node's forward signal with SWIPT-PS technique, $\sqrt{P_j^t} h x_j(m)$ is the signal transmitted with DL, P_j^t (or P_i^t) is the transmit power of node S_j (or S_i), and n_i is the additive Gaussian noise at node S_i. For all the noises are assumed as zero-mean symmetric complex Gaussian vector with variance σ^2. Thus, this paper omits the order numbers of the frame in the noises.

The Fig. 2b gives the signal transmission model of node R. For node R, it receives signal $x_1(m)$ and $x_2(m)$ from node S_1 and S_2, respectively. At the same time, it divides the received signal into α portion for ID and $(1-\alpha)$ portion for EH with SWIPT-PS technique. Besides the dividing operation, it also forwards the ID signal $x_r^{ID}(m)$ to node S_1 and S_2. But there is a one-frame delay from node R receiving the signals $x_1(m-1)$ and $x_2(m-1)$ till it forwarding the signals $x_r^{ID}(m)$ [12]. With SIC and MRC technique, the received signal at node R is

$$y_r(m) = \sqrt{P_i^t}h_i x_i(m) + \sqrt{P_j^t}h_j x_j(m) + \widetilde{h_{rr}}(m)x_r^{ID}(m) + n_r, \tag{4}$$

where $\sqrt{P_i^t}h_i x_i(m)$ and $\sqrt{P_j^t}h_j x_j(m)$ are signals respectively from two nodes S_i and S_j, $\widetilde{h_{rr}}(m)x_r^{ID}(m)$ is the RSI at the node R, and $x_r^{ID}(m) = \beta(\sqrt{\alpha}y_r(m-1) + n_d)$. The β is the amplification factor to maintain a constant average transmit power P_r^t at node R. The n_r and n_d are the additive Gaussian noise and the ID noise at node R.

The node R only receives signal from two end nodes and it has no signal to forward at frame 1. Thus, the received signal at node R in the frame 1 is

$$y_r(1) = \sum_{i=1}^{2} \sqrt{P_i^t}h_i x_i(1) + n_r. \tag{5}$$

In summary, Table 2 gives the signal transmission at each node for the FD-TWR-SWIPT-DL transmission strategy. At the only one time slot of every frame, node S_i transmits its signal to node R and S_j, and node R broadcasts the previous received signal from S_1 and S_2.

Substituting $x_r^{ID}(m) = \beta(\sqrt{\alpha}y_r(m-1) + n_d) = \beta(\sqrt{\alpha}(\sqrt{P_i^t}h_i x_i(m-1) + \sqrt{P_j^t}h_j x_j(m-1) + \widetilde{h_{rr}}(m-1)x_r^{ID}(m-1) + n_r) + n_d)$ into (3) and making some arrangements, then the received signal at node S_i is rewritten as

$$\begin{aligned} y_i(m) = {} & \sqrt{\alpha}\beta\sqrt{P_j^t}h_i h_j x_j(m-1) + \sqrt{P_j^t}h x_j(m) \\ & + \sqrt{\alpha}\beta h_i \widetilde{h_{rr}}(m-1)x_r^{ID}(m-1) + \sqrt{P_i^t}\widetilde{h_{ii}}(m)x_i(m) \\ & + \sqrt{\alpha}\beta\sqrt{P_i^t}h_i^2 x_i(m-1) + \sqrt{\alpha}\beta h_i n_r + \beta h_i n_d + n_i, \end{aligned} \tag{6}$$

where $\sqrt{\alpha}\beta\sqrt{P_j^t}h_i h_j x_j(m-1)$ and $\sqrt{P_j^t}h x_j(m)$ are the signals from the node S_j, $\sqrt{\alpha}\beta h_i \widetilde{h_{rr}}(m-1)x_r^{ID}(m-1)$ and $\sqrt{P_i^t}\widetilde{h_{ii}}(m)x_i(m)$ are the RSIs, $\sqrt{\alpha}\beta\sqrt{P_i^t}h_i^2 x_i(m-1)$ is the self-interference term (SIT) of node S_i, and $\sqrt{\alpha}\beta h_i n_r + \beta h_i n_d + n_i$ is the noise part. Assuming that channel reciprocity holds and perfect CSIs are available. Then, the SIT can be perfectly canceled [6]. In such case, the remaining received signal at node S_i is further rewritten as

Table 2 Signal transmission at each node

Frame	1	2	⋯	$m-1$	m
S_1 to R,S_2	$x_1(1)$	$x_1(2)$	⋯	$x_1(m-1)$	$x_1(m)$
S_2 to R,S_1	$x_2(1)$	$x_2(2)$	⋯	$x_2(m-1)$	$x_2(m)$
R to S_1,S_2		$x_r^{ID}(2)$	⋯	$x_r^{ID}(m-1)$	$x_r^{ID}(m)$

$$\begin{aligned}\overline{y_i(m)} = &\sqrt{\alpha}\beta\sqrt{P_j^t}h_i h_j x_j(m-1) + \sqrt{P_j^t}hx_j(m)\\ &+ \sqrt{\alpha}\beta h_i\widetilde{h_{rr}}(m-1)x_r^{ID}(m-1) + \sqrt{P_i^t}\widetilde{h_{ii}}(m)x_i(m)\\ &+ \sqrt{\alpha}\beta h_i n_r + \beta h_i n_d + n_i.\end{aligned} \tag{7}$$

3.1.2 Relay amplification factor

We have stated in the last subsubsection that the β is determined to maintain a constant average transmit power P_r^t at node R. With the relay amplification factor β, we can get the following two propositions.

Proposition 1 For the FD-TWR-SWIPT-DL transmission strategy with average transmit power P_r^t at node R, the fixed relay amplification factor β is:

$$\beta = \sqrt{\frac{P_r^t}{\alpha(\sum_{i=1}^{2}P_i^t|h_i|^2 + P_r^t\Omega_r + \sigma_r^2) + \sigma_d^2}}. \tag{8}$$

Proof The amplification factor can be calculated using the following equation set:

$$x_r^{ID}(m) = \beta(\sqrt{\alpha}y_r(m-1) + n_d), \tag{9a}$$

$$x_r^{ID}(m+1) = \beta(\sqrt{\alpha}y_r(m) + n_d), \tag{9b}$$

$$\mathbb{E}\{|x_r^{ID}(m)|^2\} = \mathbb{E}\{|x_r^{ID}(m+1)|^2\} = P_r^t, \tag{9c}$$

$$\mathbb{E}\{|y_r(m)|^2\} = \sum_{i=1}^{2}P_i^t|h_i|^2 + \Omega_r\mathbb{E}\{|x_r^{ID}(m)|^2\} + \sigma_r^2. \tag{9d}$$

The (9a) and (9b) describe the relay amplification at frame m and $m+1$; The (9c) shows the total transmit power constraint of node R with P_r^t; The (9d) comes directly from (4). After solving the (9a), (9b), (9c), and (9d), we can obtain the (8). The proof is completed. □

The Proposition 1 implies that for the amplification factor given in (8), once the average transmit power is P_r^t at the initial frame, it will remain unchanged. In the following proposition, we show that even if the average transmit power at the initial frame is not equal to P_r^t, it will converge to P_r^t finally.

Proposition 2 For the FD-TWR-SWIPT-DL transmission strategy with the relay amplification factor given in (8) and $\mathbb{E}\{|y_r(1)|^2\} = \sum_{i=1}^{2}P_i^t|h_i|^2 + \sigma_r^2 = c$, $\beta^2 c \neq P_r^t$, the average transmit power at the relay node $\mathbb{E}\{|x_r^{ID}(m)|^2\}$ has the following property:

$$\lim_{m\to\infty}\mathbb{E}\{|x_r^{ID}(m)|^2\} = P_r^t. \tag{10}$$

Proof Based on the (9a) and (9d), the average received power of two consecutive frames has the following relation:

$$\mathbb{E}\{|y_r(m)|^2\} = \sum_{i=1}^{2} P_i^t |h_i|^2 + \Omega_r \beta^2 (\alpha \mathbb{E}\{|y_r(m-1)|^2\} + \sigma_d^2) + \sigma_r^2. \tag{11}$$

As $\mathbb{E}\{|y_r(1)|^2\} = c$, it can be shown that

$$\begin{aligned} \mathbb{E}\{|y_r(m)|^2\} = &\sum_{i=1}^{2} P_i^t |h_i|^2 + P_r^t \Omega_r + \sigma_r^2 \\ &+ \frac{(c - \sum_{i=1}^{2} P_i^t |h_i|^2 - P_r^t \Omega_r - \sigma_r^2)(\alpha P_r^t \Omega_r)^{m-1}}{(\alpha(\sum_{i=1}^{2} P_i^t |h_i|^2 + P_r^t \Omega_r + \sigma_r^2) + \sigma_d^2)^{m-1}}. \end{aligned} \tag{12}$$

As $\alpha(\sum_{i=1}^{2} P_i^t |h_i|^2 + P_r^t \Omega_r + \sigma_r^2) + \sigma_d^2 = \alpha P_r^t \Omega_r + (\alpha \sum_{i=1}^{2} P_i^t |h_i|^2 + \alpha\sigma_r^2 + \sigma_d^2)$, and $(\alpha \sum_{i=1}^{2} P_i^t |h_i|^2 + \alpha\sigma_r^2 + \sigma_d^2) > 0$, thus $0 < \frac{\alpha P_r^t \Omega_r}{\alpha(\sum_{i=1}^{2} P_i^t |h_i|^2 + P_r^t \Omega_r + \sigma_r^2) + \sigma_d^2} < 1$ can be found, then the following equation can be further obtained

$$\lim_{m \to \infty} \mathbb{E}\{|y_r(m)|^2\} = \sum_{i=1}^{2} P_i^t |h_i|^2 + P_r^t \Omega_r + \sigma_r^2. \tag{13}$$

Thus, we have

$$\begin{aligned} \lim_{m \to \infty} \mathbb{E}\{|x_r^{ID}(m)|^2\} &= \beta^2 (\alpha \lim_{m \to \infty} \mathbb{E}\{|y_r(m-1)|^2\} + \sigma_d^2) \\ &= P_r^t. \end{aligned} \tag{14}$$

The proof is completed. □

3.1.3 Transmission strategy analysis

With (7), the instantaneous received signal to interference plus noise ratio (SINR) of the FD-TWR-SWIPT-DL transmission strategy at node S_i is

$$\gamma_i = \frac{\alpha\beta^2 P_j^t |h_i|^2 |h_j|^2 + P_j^t |h|^2}{\alpha\beta^2 P_r^t |h_i|^2 \Omega_r + P_i^t \Omega_i + \alpha\beta^2 |h_i|^2 \sigma_r^2 + \beta^2 |h_i|^2 \sigma_d^2 + \sigma_i^2}. \tag{15}$$

With (1), (15), and Shannon capacity formula, the specific total capacity of the FD-TWR-SWIPT-DL transmission strategy is

$$C_t = C_1 + C_2 = \sum_{i=1}^{2} T^t W \log_2(1 + \gamma_i), \tag{16}$$

where W is bandwidth.

With (2), the specific total energy consumption of the FD-TWR-SWIPT-DL transmission strategy is

$$E_t = T^t(\epsilon(P_1^t + P_2^t) + P^c), \tag{17}$$

where the total transmit power of the FD-TWR-SWIPT-DL transmission strategy is $P^t = P_1^t + P_2^t$. The total circuit power of the FD-TWR-SWIPT-DL transmission strategy is $P^c = \sum_{i=1}^{2}(P_i^{ct} + P_i^{cr} + P_i^{c\varsigma} + P_i^{cs})$. The P_i^{ct}, P_i^{cr}, P_i^{cs}, and $P_i^{c\varsigma}$ respectively represent transmit, receive, SIC and SIT circuit powers of node S_i. This paper considers the linear circuit power consumption model and we can consider the nonlinear one in our future work.

From (17), we can know that the E_t does not contain the power consumption of relay node. Because the relay node forwards signal with SWIPT-PS technique, which means it can harvest energy from the received signal.

With (4), the harvested energy of the FD-TWR-SWIPT-DL transmission strategy at node R is

$$E_h = T^t\zeta(1-\alpha)\left(\sum_{i=1}^{2} P_i^t|h_i|^2 + P_r^t\Omega_r + \sigma_r^2\right), \tag{18}$$

where ζ is a constant for the harvesting efficiency.

For node R is considered battery limited, the following inequality also should always be met

$$E_h \geq T^t(P_r^t + P_r^c), \tag{19}$$

where $P_r^c = P_r^{ct} + P_r^{cr} + P_r^{cs} + P_r^{c\varsigma}$ is the total circuit power of node R. The P_r^{ct}, P_r^{cr}, P_r^{cs}, and $P_r^{c\varsigma}$ respectively represent transmit, receive, SIC and SIT circuit powers of node R. All the circuit powers are static powers with a constant value and the circuit powers are from 0 to serval hundreds of mw [25], i.e., $\{P_i^{ct}, P_i^{cr}, P_i^{cs}, P_i^{c\varsigma}, P_r^{ct}, P_r^{cr}, P_r^{cs}, P_r^{c\varsigma}\} \in (0, 800)$ mw. In such case, P_r^c and P^c are also constants can be further obtained.

From (19), we can know that the relay node can get its energy consumption with SWIPT-PS technique. This also gives the reason of the networks' lifetime extended. Without the SWIPT-PS technique and (19), the networks outages for the energy-constrained relay node.

With (16)–(17) and the definition of EE, the EE of the FD-TWR-SWIPT-DL transmission strategy can be written as

$$\eta = \frac{\sum_{i=1}^{2} T^t W \log_2(1+\gamma_i)}{T^t(\epsilon(P_1^t + P_2^t) + P^c)} = \frac{\sum_{i=1}^{2} W \log_2(1+\gamma_i)}{\epsilon(P_1^t + P_2^t) + P^c}. \tag{20}$$

3.1.4 HD two-way AF relaying

To show the effectiveness of the FD-TWR-SWIPT-DL transmission strategy, we also give the EE of the traditional HD two-way AF relaying [6]. In the traditional HD two-way AF relaying, two source nodes complete a bidirectional communication process with physical layer encoding [28]. In such case, we set $\Omega_1 = \Omega_2 = \Omega_r = 0, \alpha = 1$, and we also don't consider DL, then γ_i turns into the SNR of the HD two-way AF relaying γ_i' at two source nodes

$$\gamma_i' = \frac{P_r^t P_j^t |h_i|^2 |h_j|^2}{P_j^t |h_i|^2 \sigma_i^2 + P_i^t |h_i|^2 \sigma_i^2 + P_r^t |h_i|^2 \sigma_r^2 + \sigma_i^2 \sigma_r^2}. \tag{21}$$

Then the total capacity of the HD two-way AF relaying is

$$C_t' = \frac{1}{2} T^t W \sum_{i=1}^{2} \log_2(1+\gamma_i'). \tag{22}$$

The total capacity is halved, because the signal transmission is completed in two time slots with HD transmission.

The total energy consumption of the HD two-way AF relaying is

$$E_t' = \frac{1}{2} T^t (\epsilon(P_1^t + P_2^t + P_r^t) + P^{c'}), \tag{23}$$

where $P^{c'} = \sum_{i=1}^{2}(P_i^{ct} + P_i^{cr} + P_i^{cs}) + P_r^{ct} + P_r^{cr}$ is the total circuit power of the HD two-way AF relaying. The $P^{c'}$ contains the P_r^{ct} and P_r^{cr}. At the same time, different from the FD-TWR-SWIPT-DL transmission strategy, the total energy consumption of the HD two-way AF relaying also contains P_r^t without SWIPT.

Finally, with (22)–(23) and the definition of EE, the EE of the HD two-way AF relaying can be further given as

$$\eta' = \frac{\frac{1}{2} T^t W \sum_{i=1}^{2} \log_2(1+\gamma_i')}{\frac{1}{2} T^t (\epsilon(P_1^t + P_2^t + P_r^t) + P^{c'})} = \frac{W \sum_{i=1}^{2} \log_2(1+\gamma_i')}{\epsilon(P_1^t + P_2^t + P_r^t) + P^{c'}}. \tag{24}$$

3.2 EE maximization problems and analyses

In this subsection, we give the EE maximization problems and analyses of the designed transmission strategy with EPA and OPA.

3.2.1 Equal power allocation

Firstly, we discuss the EE maximization problem with EPA. With EPA, it means $P_1^t = P_2^t = P_r^t = P$, then we can obtain the following proposition.

Proposition 3 With EPA, i.e., $P_1^t = P_2^t = P_r^t = P$, when the transmit power P approaches infinity, C_t has no relation with PS factor α and C_t has an upper bound:

$$\lim_{P\to\infty} C_t = \sum_{i=1}^{2} T^t W \log_2 \left(1 + \frac{|h_i|^2 |h_j|^2 + |h|^2(|h_i|^2 + |h_j|^2 + \Omega_r)}{|h_i|^2 \Omega_r + \Omega_i(|h_i|^2 + |h_j|^2 + \Omega_r)}\right). \tag{25}$$

Proof It's straightforward that

$$\lim_{P\to\infty} C_t = \sum_{i=1}^{2} T^t W \log_2(1 + \lim_{P\to\infty} \gamma_i). \tag{26}$$

Then we can obtain the (25).

The proof is completed. □

From (25), we can find that the C_t has no relation with α. At the same time, the Proposition 3 implies that RSI restricts the performance of the FD two-way AF relaying. This is quite different from the HD two-way AF relaying. For the HD two-way AF relaying with (21) and (22), we can know that if the transmit power goes to infinity, the capacity also goes to infinity. However, with the FD technique, there exists the limit of capacity due to RSI.

With (16)–(17) and the definition of EE, the EE of the FD-TWR-SWIPT-DL transmission strategy with EPA is

$$\eta_e = \frac{\sum_{i=1}^{2} T^t W \log_2\left(1+\frac{\alpha\beta^2 P|h_i|^2|h_j|^2+P|h|^2}{\alpha\beta^2 P|h_i|^2\Omega_r+P\Omega_i+\alpha\beta^2|h_i|^2\sigma_r^2+\beta^2|h_i|^2\sigma_d^2+\sigma_i^2}\right)}{T^t(2\epsilon P+P^c)}, \tag{27}$$

where $C_{te}=\sum_{i=1}^{2} T^t W\log_2\left(1+\frac{\alpha\beta^2 P|h_i|^2|h_j|^2+P|h|^2}{\alpha\beta^2 P|h_i|^2\Omega_r+P\Omega_i+\alpha\beta^2|h_i|^2\sigma_r^2+\beta^2|h_i|^2\sigma_d^2+\sigma_i^2}\right)$, $E_{te}=T^t(2\epsilon P+P^c)$, and $\beta^2=\frac{P}{\alpha(\sum_{i=1}^{2}P|h_i|^2+P\Omega_r+\sigma_r^2)+\sigma_d^2}$.

With EPA, we aim to maximize EE by jointly optimizing the transmit power P and the PS ratio α under individual capacity requirements, the maximum transmit power constraints, and the EH constraints. Finally, with (27), the EE maximization problem is

$$\max_{\alpha,P} \ \eta_e \quad \text{s.t. } C_i \geq C_{i,\min}, \tag{28a}$$

$$0 \leq \{P\} \leq P_t^{\max}, \tag{28b}$$

$$E_{he} \geq T^t(P+P_r^c), \tag{28c}$$

$$\text{and } 0<\alpha<1, \tag{28d}$$

where $E_{he}=T^t\zeta(1-\alpha)(2P|h_i|^2+P\Omega_r+\sigma_r^2)$, $C_{i,\min}$ is the minimum required transmission task of node S_i, and $P_t^{\max}$ is the maximum allowed transmit power at nodes.

Observing the objective function of (28), we can find that it is non-convex in terms of (α, P). Since the numerator of the objective function is concave with $C_{te}''(P)<0$ and the denominator is linear, then the η_e is pseudo-concave with respect to P. At the same time, the numerator of the objective function is concave with $C_{te}''(\alpha)<0$, then η_e is concave with respect to α. Thus, the related optimization problem has a closed-form solution with respect to α.

With the maximization problem of η_e is determined over two variables α and P, and thus it is quite difficult to solve this problem efficiently. However, for any optimization problem, we can optimize some of the variables first, and then for the remaining ones [29]. Thus, we can divide the maximization problem of η_e into two sub-optimal problems, namely, to optimize the two variables α and P, respectively.

Firstly, we find the optimal value for α while fixing P. With the given P, the resulting problem of η_e is monotonically increasing and hence we can get the optimal value of the α as

$$\alpha^{opt} = 1 - \frac{P + P_r^c}{\zeta(P|h_1|^2 + P|h_2|^2 + P\Omega_r + \sigma_r^2)}. \tag{29}$$

Substituting the α^{opt} into (27), the objective function of (28) is only determined by the variable P. Then we apply a convex optimization method to optimize the pseudo-concave function with respect to P. In order to tackle this problem, we can further employ the Dinkelbach's algorithm to get the solution of concave–convex fractional programming [30]. Then we can express the objective function of (28) with respect to P as $\frac{f(x)}{g(x)}$, where $f(x)$ is concave and $g(x)$ is linear.

Define the function $F(\psi)$ as $F(\psi) = \max_{x\in S}\{f(x) - \psi g(x)\}$ with continuous and positive f, g, and compact S. Then $F(\psi)$ is convex with respect to ψ, $F(\psi)$ is strictly decreasing and it has a unique root ψ^*. At the same time, the problem of finding $F(\psi)$ can be solved with convex optimization approaches, and it is shown that the problem of maximizing $\frac{f(x)}{g(x)}$ is equivalent to finding ψ^* [30]. For each x, we can make a summary of the Dinkelbach's algorithm as Algorithm 1, where the superscript (n) denotes the number of iteration. With the Algorithm 1, it leads to the optimal values of a pseudo-concave function.

Based on the above analysis, we can divide the original EE maximization problem of (28) into two sub-optimal problems. At the same time, we can find that the optimal value of α has a closed-form solution with (29) and we can obtain each optimal value of P with the Algorithm 1. In such a case, we can solve the EE maximization problem of (28) in an alternating mode. In this regard, firstly, with $\alpha^{(n)}$, we adopt the fractional programming to find $P^{(n+1)}$. Secondly, with known $P^{(n+1)}$, we updates $\alpha^{(n+1)}$ with (29). Consequently, we can get the alternating optimal algorithm with EPA to optimize α and P. Algorithm 2 with EPA presents the alternating optimal procedure which updates the optimization parameters until convergence.

Algorithm 1 Dinkelbach Algorithm

1: **Set** tolerance ε, $n = 0$, and $\psi^{(n)} = 0$.
2: **Repeat**
3: $x_{opt}^{(n)} = \arg\max_{x\in S}\{f(x) - \psi^{(n)} g(x)\}$.
4: $F(\psi^{(n)}) = f(x_{opt}^{(n)}) - \psi^{(n)} g(x_{opt}^{(n)})$.
5: $\psi^{(n+1)} = \frac{f(x_{opt}^{(n)})}{g(x_{opt}^{(n)})}$.
6: $n \leftarrow n + 1$.
7: **Until** $F(\psi^{(n)}) \leq \varepsilon$.

Algorithm 2 Alternating Optimal Algorithm

1: **Set** initial points $\alpha^{(0)}$, $P_1^{t(0)}$, $P_2^{t(0)}$, $P_r^{t(0)}$ and $n = 0$.
2: **EPA**
3: **Repeat**
4: Given $\alpha^{(n)}$, apply the Dinkelbach's algorithm to calculate $P^{(n+1)}$.
5: Compute $\alpha^{(n+1)}$ in (29).
6: $n \leftarrow n + 1$.
7: **Until** Convergence.
8: **OPA**
9: **Repeat**
10: Given $\alpha^{(n)}$, $P_r^{t(n)}$, and $P_2^{t(n)}$, apply the Dinkelbach's algorithm to calculate $P_1^{t(n+1)}$.
11: Given $\alpha^{(n)}$, $P_r^{t(n)}$, and $P_1^{t(n+1)}$, apply the Dinkelbach's algorithm to calculate $P_2^{t(n+1)}$.
12: Compute $\alpha^{(n+1)}$ in (32).
13: Compute $P_r^{t(n+1)}$ in (33).
14: $n \leftarrow n + 1$.
15: **Until** Convergence.

Next, we give the computational complexity of Algorithm 2 with EPA. To analyze the computational complexity of Algorithm 2 with EPA, we can find that the Algorithm 2 employs Algorithm 1. But the convergence rate of Algorithm 1 is independent of the complexity of finding $x_{opt}^{(n)}$ for its super linear convergence. As the problems of finding $x_{opt}^{(n)}$ in Algorithm 2 are convex, their complexity can be modeled in polynomial form in terms of the number of variables and constraints. With these properties, we can give the complexity of Algorithm 2. The complexities with step 4 to step 5 are respectively $\mathcal{O}(1)$ and $\mathcal{O}(11)$. Then, with EPA, the total complexity of Algorithm 2 for one iteration is $\mathcal{O}(\mathcal{I}_{d_1} + 11)$, where $\mathcal{I}_{d_1}$ is the required number of iteration with step 4.

3.2.2 Optimal power allocation

Secondly, we discuss the EE maximization problem with OPA. With the OPA, the similar proposition like Proposition 3 can also be obtained when the transmit powers P_1^{topt}, P_2^{topt}, and P_r^{topt} approaches infinity.

Proposition 4 With OPA, when the transmit powers P_1^{topt}, P_2^{topt}, and P_r^{topt} approaches infinity, C_t has no relation with PS factor α and C_t has an upper bound:

$$\lim_{P_1^{topt}, P_2^{topt}, P_r^{topt} \to \infty} C_t = \sum_{i=1}^{2} T^t W \log_2 \left(1 + \frac{|h_i|^2 |h_j|^2 + |h|^2 (|h_i|^2 + |h_j|^2 + \Omega_r)}{|h_i|^2 \Omega_r + \Omega_i (|h_i|^2 + |h_j|^2 + \Omega_r)} \right). \quad (30)$$

Proof The proof is omitted for it's the same like Proposition 3.

The proof is completed.

The reason of the Proposition 4 is the same as the Proposition 3. That is there exists the limit of capacity due to the RSI for the FD two-way AF relaying.

With the OPA, we aim to maximize EE by jointly optimizing the transmit power P_1^t, P_2^t, P_r^t, and the PS ratio α under constraints. Then with (20), the EE maximization problem is

$$\max_{\alpha,P_1^t,P_2^t,P_r^t} \quad \eta \tag{31a}$$

$$\text{s.t. } C_i \geq C_{i,\min}, \tag{31a}$$

$$0 \leq \{P_1^t, P_2^t, P_r^t\} \leq P_t^{\max}, \tag{31b}$$

$$E_h \geq T^t(P_r^t + P_r^c), \tag{31c}$$

$$\text{and } 0 < \alpha < 1. \tag{31d}$$

The objective function of (31) is non-convex in terms of $(\alpha, P_1^t, P_2^t, P_r^t)$. Since the numerator of the objective function is respectively concave with $C_t''(P_1^t) < 0$ and $C_t''(P_2^t) < 0$, and the denominator is linear, then the η is respectively pseudo-concave with respect to P_1^t and P_2^t. At the same time, the numerator of the objective function is respectively concave with $C_t''(P_r^t) < 0$ and $C_t''(\alpha) < 0$, then the η is respectively concave with respect to P_r^t and α. Similar to EPA, the related optimization problem has a closed-form solution with respect to P_r^t and α. We can also divide the original problem into four sub-optimal problems, namely, to optimize the four variables α, P_1^t, P_2^t, and P_r^t, respectively.

Firstly, we find the optimal value for α while fixing other variables with the objective function of (31). In such a case, considering that all the variables except α are given, then the resulting EE problem is monotonically increasing and hence we can get the optimal value of the α as

$$\alpha^{opt} = 1 - \frac{P_r^t + P_r^c}{\zeta(P_1^t|h_1|^2 + P_2^t|h_2|^2 + P_r^t\Omega_r + \sigma_r^2)}. \tag{32}$$

With the fixed α, we can further obtain the optimal P_r^t with the following formula

$$P_r^{topt} = \frac{\zeta(1-\alpha^{opt})(P_1^t|h_1|^2 + P_2^t|h_2|^2 + \sigma_r^2) - P_r^c}{1 - \zeta(1-\alpha^{opt})\Omega_r}. \tag{33}$$

At the same time, we can get the other optimal variables P_1^t and P_2^t with Dinkelbach's algorithm like EPA.

In this regard, firstly, with $\alpha^{(n)}$, $P_r^{t(n)}$, and $P_2^{t(n)}$, we adopt the fractional programming to find $P_1^{t(n+1)}$. Secondly, with known $\alpha^{(n)}$, $P_r^{t(n)}$, and $P_1^{t(n+1)}$, we can find $P_2^{t(n+1)}$. Thirdly, with known $P_1^{t(n+1)}$, $P_2^{t(n+1)}$ and $P_r^{t(n)}$, we can update $\alpha^{(n+1)}$ with (32). Lastly, with known $P_1^{t(n+1)}$, $P_2^{t(n+1)}$ and $\alpha^{(n+1)}$, we can update $P_r^{t(n+1)}$ with (33). Consequently, we can get the alternating optimal algorithm with OPA to optimize α, P_1^t, P_2^t, and P_r^t. Algorithm 2 with OPA presents the alternating optimal procedure which updates the optimization parameters until convergence.

Finally, like EPA, we give the computational complexity of Algorithm 2 with OPA. The complexities from step 10 to step 11 are all $\mathcal{O}(1)$, and the complexities from step 12 to step 13 are respectively $\mathcal{O}(11)$ and $\mathcal{O}(12)$. Then, with OPA, the total complexity of Algorithm 2 for one iteration is $\mathcal{O}(\mathcal{I}_{d_2} + \mathcal{I}_{d_3} + 11 + 12)$, where $\mathcal{I}_{d_2}$ and $\mathcal{I}_{d_3}$ are respectively the required number of iterations from step 10 to step 11.

4 Results and discussion

In this section, we give the simulations to evaluate the SE and EE of the FD-TWR-SWIPT-DL transmission strategy. Table 3 specifies the simulation parameters. In the figures of the simulation, we express the FD-TWR-SWIPT-DL transmission strategy as FD-1TS-EH and the traditional HD two-way AF relaying as HD-2TS [6]. For a better comparison, we also give the EE of the FD-TWR-SWIPT-DL transmission strategy without EH requirements (namely FD-1TS in the figures). In the simulations, the powers are optimal allocated. At the same time, we set the parameters based on the existing work [23] and [25]. Thus, $\nu = 4$, $\alpha = 0.8$, $P_i^{ct} = P_i^{cr} = 50$ mW, $P_i^{cs} = 80$ mW, $P_j^{c\varsigma} = 30$ mW, and $\Omega_i = \Omega_r = \Omega$ will be considered without special explanation.

In this section, we first give the outage probabilities with EPA and OPA. We give the outage probabilities rather than transmission rates, for the similar characteristics of transmission rates and outage probabilities, and the higher transmission rates usually means the lower outage probabilities. At the same time, the outage probabilities can show the differences of EPA and OPA from a different perspectives.

Figure 3 shows the outage probabilities with EPA and OPA. From Fig. 3, we can get the following results: (i)The outage probabilities of OPA are lower than that of EPA in three transmission schemes, which shows the effectiveness of OPA. (ii) No matter with OPA or EPA, the outage probability of FD-1TS is the best and the outage probability of HD-2TS is the worst. This is for the FD-1TS has the advantages of FD technique, DLs, and it also has no energy constrained node. These three characteristics make the highest transmission rate of FD-1TS, which finally result in the best outage probability. The HD-2TS has the worst outage probability, for it works in HD technique, and it also has no DL. (iii) When the SNR is high, no matter with EPA or OPA, the outage probabilities of FD-1TS-EH and FD-1TS are the same. Because when the SNR is high, the transmission rates of this two schemes are the same. This phenomenon can also be seen in the following figures.

Table 3 Simulation parameters

Symbol	Definition	Values
σ^2	Noise power	−94 dBm
T^t	Frame duration	5 ms
W	System bandwidth	10 MHz
$C_{i,\min}$	QoS requirements	(0, 0.25] Mbits
ν	Path-loss exponent	[2−4]
$P_i^{c\varsigma}, P_r^{c\varsigma}$	SIT circuit power	[0, 800) mW
P_i^{cs}, P_r^{cs}	SIC circuit power	[0, 800) mW
P_i^{ct}, P_r^{ct}	Transmit circuit power	[0, 800) mW
P_i^{cr}, P_r^{cr}	Receive circuit power	[0, 800) mW
α	Information decoding factor	0−1
ζ	Harvesting efficiency	0.8
$1/\epsilon$	Power amplifier efficiency	1/0.38
Ω_i, Ω_r	Average power gains of RSI channels	0–10
$P_t^{\max}$	Maximum transmit power	70 dBm

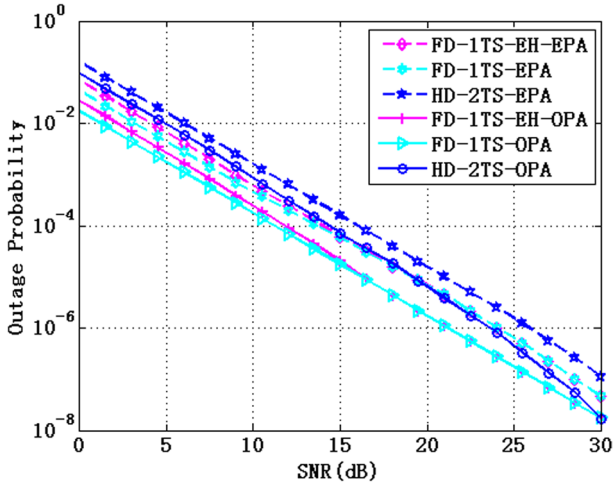

Fig. 3 Outage probabilities with EPA and OPA

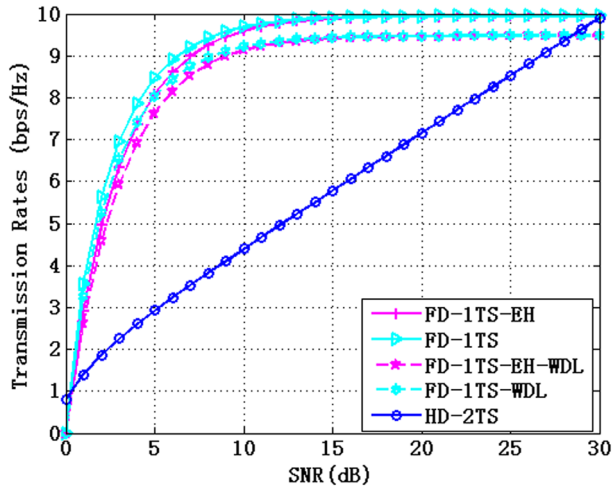

Fig. 4 Transmission rates with and without DLs

Figure 4 shows the transmission rates with and without DLs (WDL). In Fig. 4, the transmission rates of FD-1TS-EH and FD-1TS are respectively higher than that of FD-1TS-EH-WDL and FD-1TS-WDL. The FD-1TS-EH-WDL is our designed transmission strategy without the consideration of DLs. This phenomenon shows the SE gain of our proposed transmission strategy with the consideration of DLs. At the same time, the transmission rate of FD-1TS is a little higher than our FD-1TS-EH. Because the FD-1TS has no energy-constrained node and it can use more power for signal transmission to get the higher transmission rate. Except for this two phenomena, when the SNR is high, we can also get the other two results: (i) No matter with or without DLs, the transmission rates of FD-1TS-EH and FD-1TS are the same. Because when the SNR is high, the influence of the energy-constrained node is very

small, which results in the same transmission rates of FD-1TS and FD-1TS-EH. (ii) For the FD system with RSI, the transmission rates of FD-1TS-EH and FD-1TS will saturate for large SNR. This phenomenon is corresponding to the Proposition 4.

Figure 5 shows the transmission rates with different Ω. From Fig. 5, we can get two results: (i) As the Ω increases, the transmission rates of our FD-1TS-EH decrease; (ii) When the Ω exceeds a certain level, the HD-2TS's transmission rate even outperforms the FD system. The reason of this two results is for the RSI decreases the transmission rates of the FD system. This phenomenon is also corresponding to the Proposition 4. With the technological progress in SIC techniques, we consider the $\Omega = 0.1$ [19] in the other figures.

Figure 6 shows the transmission rates with different transmission schemes. In Fig. 6, we give the transmission rates of FD-TWR-2TS and FD-TWR-1TS transmission strategies in [12] (namely FD-2TS-[12] and FD-1TS-[12] in the figures). This two transmission strategies also can respectively complete the bidirectional communication in only two time slots and one time slot with FD technique. The transmission rates of FD-2TS-[12], FD-1TS-[12], and HD-2TS in Fig. 6 are given as a benchmark to show the SE gain of our proposed transmission strategy. At the same time, to give a comparison with the simulation results, we also give the numerical result of our FD-1TS-EH (namely FD-1TS-EH-N in the figures).

From Fig. 6, we can get the following results: (i) The transmission rates of FD-2TS-[12] and FD-1TS-[12] are lower than our FD-1TS-EH. Because our proposed transmission strategy can complete the bidirectional communication in only one time slot with the consideration of the DLs. (ii) The transmission rates of FD-1TS-EH-N is close to our FD-1TS-EH. This phenomenon shows the effectiveness of the theoretical analysis.

Based on the above transmission rates, we next give the comparisons of EEs.

Figure 7 shows the EEs with zero circuit powers (ZCP) and non-zero circuit powers (NCP) situations. In ZCP situation, all the circuit powers are zero, thus $P_r^c = P^c = 0$. In NCP situation, $\{P_i^{ct}, P_r^{ct}, P_i^{cr}, P_r^{cr}, P_i^{cs}, P_r^{cs}, P_i^{cs}, P_r^{cs}, \} \in (0, 800)$ mW. From Fig. 7,

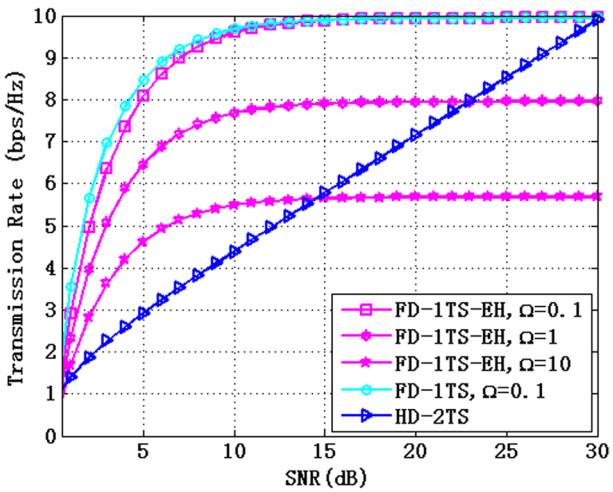

Fig. 5 Transmission rates with different Ω

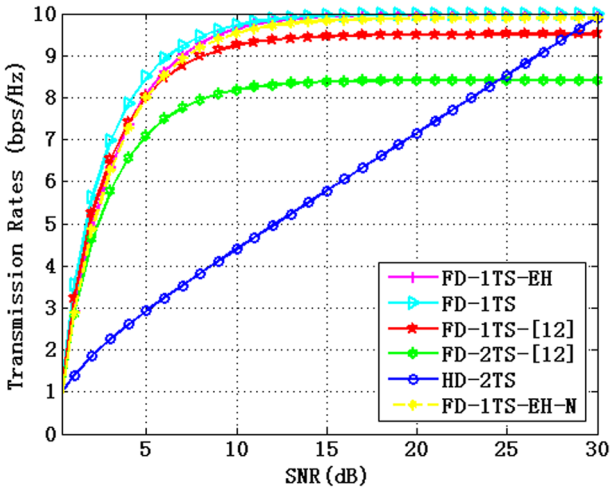

Fig. 6 Transmission rates with different transmission schemes

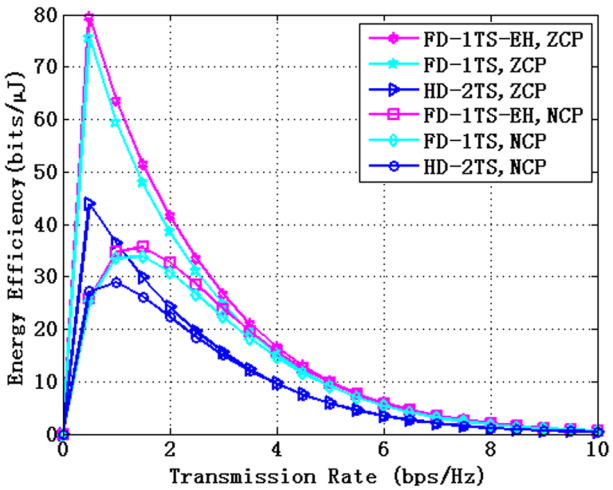

Fig. 7 EEs with ZCP and NCP

we can get two results: (i) No matter in ZCP or NCP situation, the EE of our FD-1TS-EH is the highest and the EE of HD-2TS is the lowest, which shows the EE gain of our FD-1TS-EH. Although the transmission rate of FD-1TS in Fig. 6 is the highest, but for our FD-1TS-EH doesn't need to consider the P_r^t and P_r^c, thus its EE is the highest. (ii) When the transmission rate is low, the EEs of ZCP situation are higher than that of NCP situation in three transmission schemes. This is for circuit powers make a greater influence on EE with low transmission rate when comparing with transmit power. But when the transmission rates are high, the transmit powers are much bigger than that of circuit power. Thus, the EEs of ZCP and NCP situations are the same.

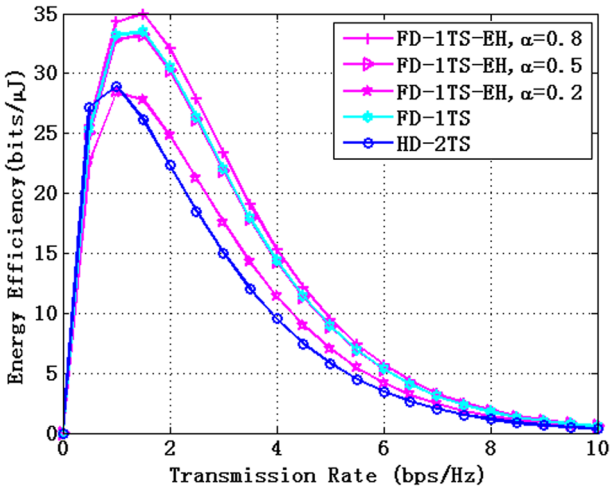

Fig. 8 EEs with different α

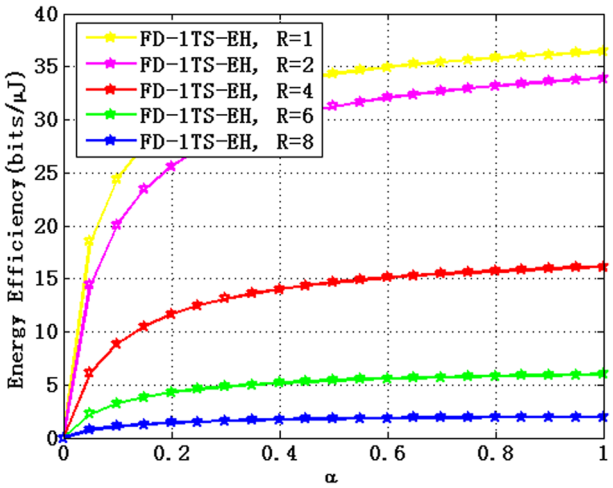

Fig. 9 EEs with different transmission rates

Figure 8 shows the EEs with different α. From Fig. 8, we can find that the bigger the α, the higher the EEs for our FD-1TS-EH. This is corresponding to the concave characteristics of $\eta(\alpha)$. Thus, the EE of our FD-1TS-EH increases with the increasing of α.

Figure 9 shows the EEs of our FD-1TS-EH with different transmission rates. From Fig. 9, we can find that the increases of our FD-1TS-EH's EE is not significant with the bigger α. Although our FD-1TS-EH must meet the EH requirements, this phenomenon shows that the EH requirements will not make a great influence on the EE of our FD-1TS-EH when the α is big. At the same time, the total energy consumption of our FD-1TS-EH does not need to contain the P_r^t and P_r^c. Both of this two reasons explain why our FD-1TS-EH has the highest EE in the other figures.

Figure 10 shows the EEs with EPA and OPA. From Fig. 10, we can find that the EE of our FD-1TS-EH with OPA is the highest and the EE of HD-2TS with EPA is the lowest. Because our FD-1TS-EH has FD advantage, DLs advantage, and it can harvest

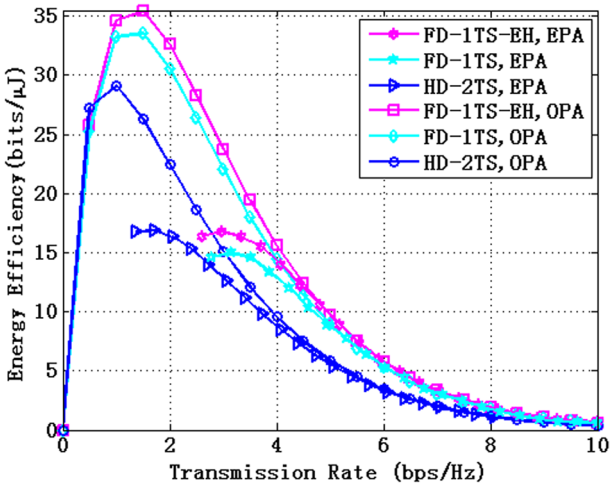

Fig. 10 EEs with EPA and OPA

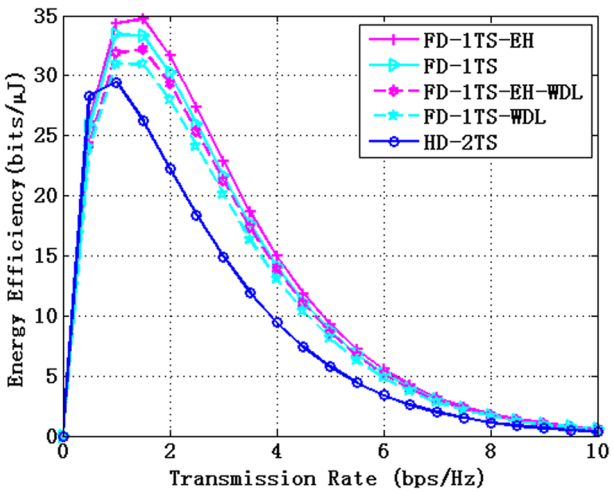

Fig. 11 EEs with and without DLs

energy with SWIPT-PS without the consideration of P_r^t and P_r^c. At the same time, we can find that the EEs of OPA are higher than that of EPA in three transmission schemes. This phenomenon also shows the significance of OPA.

Figure 11 shows the EEs with and without DLs. In Fig. 11, the EEs of FD-1TS-EH and FD-1TS are respectively higher than that of FD-1TS-EH-WDL and FD-1TS-WDL. This phenomenon shows the EE gain of our proposed transmission strategy with the consideration of DLs.

Figure 12 shows the EEs with different Ω. From Fig. 12, we can find that the bigger the Ω, the lower the EEs of our FD-1TS-EH. At the same time, when $\Omega = 10$, the EE of our FD-1TS-EH is even worse than that of HD-2TS. Both of this two phenomena show the importance of SIC with FD technique.

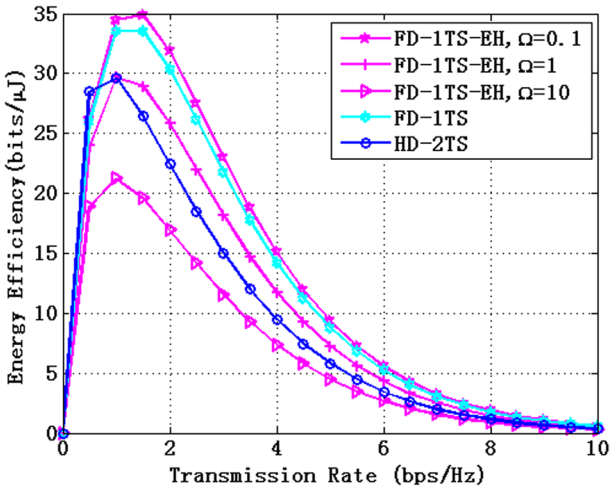

Fig. 12 EEs with different Ω

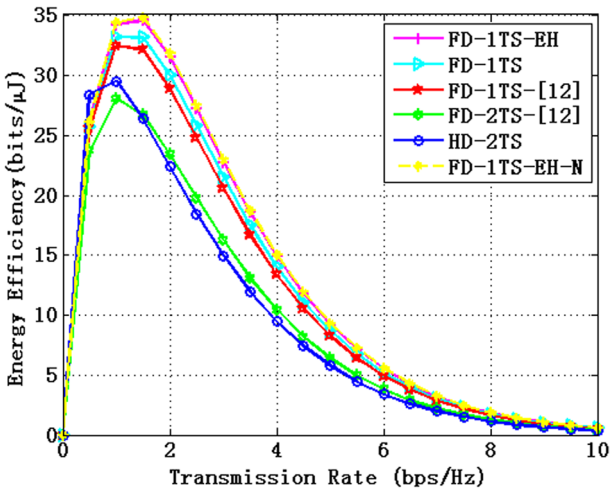

Fig. 13 EEs with different transmission schemes

Figure 13 shows the EEs with different transmission schemes. In Fig. 13, the EEs of FD-2TS-[12], FD-1TS-[12], and HD-2TS are given as a benchmark to show the EE gain of our proposed transmission strategy. From Fig. 13, firstly, the EE of FD-1TS-EH-N is close to our FD-1TS-EH. This phenomenon also shows the effectiveness of the theoretical analysis. Secondly, the EEs of FD-2TS-[12] and FD-1TS-[12] are lower than that of FD-1TS and our FD-1TS-EH. Because the FD-2TS-[12] and FD-1TS-[12] did not consider the DLs with the same power consumption. At the same time, to simplify analysis, the [12] assumed all the signals forwarded by relay as unit signals. Both of this two reasons reduce the transmission rates and EEs of them.

Figure 14 shows the convergence behavior of our proposed algorithm and its required number of iterations for 6 different initial points. This figure confirms that different initial points converge to one fixed point with almost 4 times of iterations, which shows the effectiveness of the proposed algorithm.

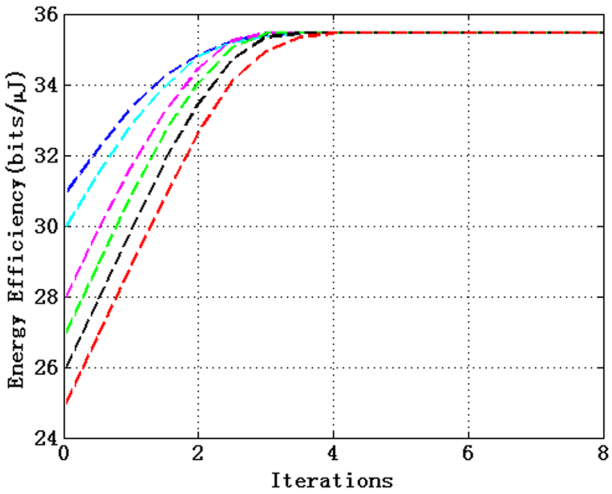

Fig. 14 Convergence behavior of the FD-1TS-EH with different initial points

5 Conclusion

In this paper, we have designed a FD-TWR-SWIPT-DL transmission strategy to improve networks' SE, to extend networks' lifetime, and to maximize networks' EE. With the FD-TWR-SWIPT-DL transmission strategy, a bidirectional communication with the consideration of DLs has been completed in only one time slot to achieve the higher SE transmission. At the same time, the networks' lifetime has been extended with the relay node transmits signal with SWIPT. In addition, the networks' EE has been maximized by our proposed alternating optimal algorithm. The simulations have shown the SE and EE advantages of our FD-TWR-SWIPT-DL transmission strategy, which indicates the effectiveness of our FD-TWR-SWIPT-DL transmission strategy. At last, multiple-antenna technique can be more effectively to improve networks' SE and EE. Thus, the EE maximization problem of energy-constrained FD relay networks with multiple-antenna transmission can be discussed in the future work.

Abbreviations

EH	Energy harvesting
SWIPT	Simultaneous wireless information and power transfer
TS	Time-switching
PS	Power-splitting
ID	Information decoding
EE	Energy efficiency
SE	Spectral efficiency
TWR	Two-way relaying
HD	Half-duplex
FD	Full-duplex
SIC	Self-interference cancellation
DL	Direct link
CSI	Channel state information
OPA	Optimal power allocation
EPA	Equal power allocation
AF	Amplify-and-forward
RSI	Residual self-interference
MRC	Maximum ratio combining
SINR	Signal to interference plus noise ratios
SIT	Self-interference terms

QoS Quality of service
ZCP Zero circuit powers
NCP Non-zero circuit powers

Acknowledgements
The authors would like to thank Dr. Fengde Jia from Donghua University for very valuable assistance and helpful discussions on carrying out the ideas, analysis and performance evaluation related to this work. And thank Prof. Xiaoyan Xu from Shanghai Maritime University, Prof. Xue-Qin Jiang from Donghua University, and Prof. Runhe Qiu from Donghua University for their helpful comments, suggestions and assistance in conceiving this work. Thanks very much for the Prof. Shengli Zhang of Shenzhen University to improve the quality of this paper.

Author contributions
The main contributions of CC, FZ, HH, WG, and YY were to create the main ideas, perform theoretical analysis, and execute performance evaluation by extensive simulation while MC, and BS worked as the advisors to discuss, create, and advise the main ideas and performance evaluations together.

Funding
This research was supported in part by the National Nature Science Foundation of China Project under Grant 62102466, Grant 52371331, Grant 52271321, and Grant 52101362. And it was early supported in part by the National Nature Science Foundation of China Project under Grant 61801106 and U1706224.

Availability of data and materials
Data sharing is not applicable to this article as no datasets were generated or analyzed during the current study.

Declarations

Competing interests
The authors declare that they have no known competing financial interests or personal relationships that could have appeared to influence the work reported in this paper.

Received: 21 July 2023 Accepted: 2 April 2024
Published online: 13 April 2024

References

1. H. Azarhsvs, J.M. Niya, Energy efficient resource allocation in wireless energy harvesting sensor networks. IEEE Wirel. Commun. Lett. **9**(7), 1000–1003 (2020)
2. Y. Zheng , J. Hu, K. Yang, SWIPT aided cooperative communications with energy harvesting based selective-decode-and-forward protocol: benefiting from channel aging effect. IEEE Trans. Green Commun. Netw. (2023) (**early access**)
3. D.-W. Lim, J. Kang, C.-J. Chun, H.-M. Kim, Joint transmit power and time-switching control for device-to-device communications in SWIPT cellular networks. IEEE Commun. Lett. **23**(2), 322–325 (2019)
4. H. Yang, Y. Ye, X. Chu, M. Dong, Resource and power allocation in SWIPT enabled device-to-device communications based on a non-linear energy harvesting model. IEEE Internet Things J. **7**(11), 10813–10825 (2020)
5. X. Ji, T. Wang, Energy minimization for fixed-wing UAV assisted full-duplex relaying with bank angle constraint. IEEE Wirel. Commun. Lett. 1–1 (2023) (**early access**)
6. L. Li, T. Wu, J. Qin, Sum achievable rate maximization in orbital angular momentum-based amplify-and-forward two-way relay networks. IEEE Wirel. Commun. Lett. **25**(5), 1640–1644 (2021)
7. H. Wang, Q. Yin, X.-G. Xia, Distributed beamforming for physical-layer security of two-way relay networks. IEEE Trans. Signal Process. **61**(5), 3532–3545 (2012)
8. H. Wang, F. Liu, M. Yang, Joint cooperative beamforming, jamming and power allocation to secure AF relay systems. IEEE Trans. Veh. Technol. **64**(10), 4893–4898 (2015)
9. A. Gupta, K. Singh, M. Sellathurai, Time-switching EH based joint relay selection and resource allocation algorithms for multi-user multicarrier AF relay networks. IEEE Trans. Green Commun. Netw. **3**(2), 505–522 (2019)
10. Y. Feng, V.C.M. Leung, F. Ji, Performance study for SWIPT cooperative communication systems in shadowed Nakagami fading channels. IEEE Trans. Wirel. Commun. **17**(2), 1199–1211 (2018)
11. L. Mohjazi, S. Muhaidat, M. Dianati, M. Al-Qutayri, Performance analysis of SWIPT relay networks with noncoherent modulation. IEEE Trans. Green Commun. Netw. **2**(4), 1072–1086 (2018)
12. Q. Cui, Y. Zhang, W. Ni, M. Valkama, R. Janti, Energy efficiency maximization of full-duplex two-way relay with non-ideal power amplifiers and non-negligible circuit power. IEEE Trans. Wirel. Commun. **16**(9), 6264–6278 (2017)
13. X. Zhou, Q. Li, Energy efficiency optimisation for SWIPT AF two-way relay networks. Electron. Lett. **53**(6), 436–438 (2016)
14. Y. Ye, Y. Li, Z. Wang, X. Chu, H. Zhang, Dynamic asymmetric power splitting scheme for SWIPT-based two-way multiplicative AF relaying. IEEE Signal Process. Lett. **25**(7), 1014–1018 (2018)
15. M.K. Shukla, H.H. Nguyen, O.J. Pandey, Multiuser full-duplex IoT networks with wireless-powered relaying: performance analysis and energy efficiency optimization. IEEE Trans. Green Commun. Netw. **4**(4), 982–997 (2020)
16. P. Ju, M. Wen, X. Cheng, L. Yang, Achievable-rate-enhancing self-interference cancellation for full-duplex communications. IEEE Trans. Wirel. Commun. **17**(12), 8473–8484 (2018)
17. S. Zhang, S.C. Liew, H. Wang, Blind known interference cancellation. IEEE J. Sel. Areas Commun. **31**(58), 1572–1582 (2013)

18. P. Raut, T. Kaple, P.K. Sharma, Outage and average rate performances of full-duplex multiuser AF relay systems with time-selective fading. IEEE Syst. J. **14**(3), 3390–3398 (2020)
19. M.-K. Chang, F.-T. Chien, C.-H. Kuo, Y.-C. Chen, On the accumulated loopback self-interference of two-way full-duplex AF relaying systems. IEEE Trans. Commun. **67**(5), 3167–3181 (2019)
20. D. Wang, R. Zhang, X. Cheng, L. Yang, Relay selection in two-way full-duplex energy-harvesting relay networks, in *Proceedings of 2016 IEEE Global Communications Conference (Globecom)* (Washington, 2016), pp. 1–6. https://doi.org/10.1109/GLOCOM.2016.7842211
21. D. Wang, R. Zhang, X. Cheng, L. Yang, C. Chen, Relay selection in full-duplex energy-harvesting two-way relay networks. IEEE Trans. Green Commun. Netw. **1**(2), 182–191 (2017)
22. Z. He, X. Zhang, Y. Bai, W. Jiang, Y. Rong, Optimal source and relay design for multiuser MIMO AF relay communication systems with direct links and imperfect channel information. IEEE Trans. Wirel. Commun. **15**(3), 2025–2038 (2016)
23. C. Cai, R. Qiu, X.Q. Jiang, Design and optimization for energy-efficient full-duplex transmission with direct links. IEEE Trans. Green Commun. Netw. **4**(3), 689–702 (2020)
24. Y. Jiang, C. Wan, M. Tao, F.-C. Zheng, P. Zhu, X. Gao, X. You, Analysis and optimization of fog radio access networks with hybrid caching: delay and energy efficiency. IEEE Trans. Wirel. Commun. **20**(1), 69–82 (2021)
25. C. Sun, C. Yang, Energy efficiency comparison among direct, one-way and two-way relay transmission, in *Proceedings of 2012 IEEE International Conference on Communications (ICC)* (Ottawa, 2012), pp. 4288–4293. https://doi.org/10.1109/ICC.2012.6363882
26. J. Yang, Z. He, Y. Rong, Transceiver optimization for two-hop MIMO relay systems with direct link and MSE constraints. IEEE Access **12**(11), 24203–24213 (2017)
27. X. Cheng, B. Yu, X. Cheng, L. Yang, Two-way full-duplex amplify-and-forward relaying, in *Proceedings of 2013 IEEE Military Communications Conference (Milcom)* (San Diego, 2013), pp. 1–6. https://doi.org/10.1109/MILCOM.2013.9
28. Z. Wang, L. Liu, S. Zhang, P. Dong, Q. Yang, T. Wang, PNC enabled IIoT: a general framework for channel-coded asymmetric physical-layer network coding. IEEE Trans. Wirel. Commun. **21**(12), 10335–10350 (2023)
29. J. Xu, L. Qiu, Energy efficiency optimization for MIMO broadcast channels. IEEE Trans. Wirel. Commun. **12**(2), 690–701 (2013)
30. A. Zappone, E. Jorswieck, Energy efficiency in wireless networks via fractional programming theory. Found. Trends Commun. Inf. Theory **11**(3–4), 185–396 (2015)

Publisher's Note